Mansoura Engineering Journal

Volume 24 | Issue 3 Article 1

9-1-2020

# Space/Time Analysis of Pressure Fluctuations under Spanwise and Conical Vortices.

Nabil Mostafa
*Department of Mechanical Power Engineering., Faculty of Engineering., Zagazig University., Zagazig., Egypt.*, nmostafa@vt.deu

Follow this and additional works at: https://mej.researchcommons.org/home

Recommended Citation
Mostafa, Nabil (2020) "Space/Time Analysis of Pressure Fluctuations under Spanwise and Conical Vortices.," *Mansoura Engineering Journal*: Vol. 24 : Iss. 3 , Article 1.
Available at: https://doi.org/10.21608/bfemu.1999.147934

This Original Study is brought to you for free and open access by Mansoura Engineering Journal. It has been accepted for inclusion in Mansoura Engineering Journal by an authorized editor of Mansoura Engineering Journal. For more information, please contact mej@mans.edu.eg.

# SPACE/TIME ANALYSIS OF PRESSURE FLUCTUATIONS UNDER SPANWISE AND CONICAL VORTICES

## تحليل تذبذب الضغط كدالة في الزمن و الفراغ أسفل الدوامات في اتجاه السريان و الدوامات المخروطية

*by*

**Nabil H. Mostafa**

**Department of Mechanical Power Engineering**
**Faculty of Engineering**
**Zagazig University**

**خلاصه:**

في هذا البحث درست عدد الموجات الموضعية و ترددها المتولد عن تذبذب الضغط الناتج عن نوعين من الدوامات الناتجة عن انفصال المائع عن قمة سطح نموذج ذو شكل متوازى مستطيلات. أن النوع الأول هي الدوامة المتولدة في اتجاه سريان المائع نتيجة انفصال المائع عن سطح النموذج المتعامد على اتجاه سريان المائع. و النوع الثاني هي الدوامة المتولدة بصوره مخروطية نتيجة انفصال المائع من على جانبي سطح النموذج و المائلين بزاوية ٤٥ درجه مع اتجاه سريان المائع. أن الأسلوب الذي استخدم في تقدير عدد الموجات وتردد الضغط هو عن طريق قياس و تحليل الضغط من فتحتين على سطح النموذج.

بالنسبة للدوامة المتولدة في اتجاه سريان المائع، فان القياسات قد أوضحت أن التردد و عدد الموجات المنخفض ينبئ عن تذبذب الضغط. وبمواصلة القياسات في اتجاه السريان نجد أن مستوى الطاقة قد أنخفض وانتشر في موجات ذات مستوى واسع من الترددات وعدد الموجات. كما أن في الدوامة المخروطية فان معظم الطاقة قد تركز في الموجات ذات الذبذبات المنخفضة التردد وعدد الموجات. أن عدد الموجات باختلاف ترددتها قد عرض مع اختلاف التذبذب في الضغط على سطح النموذج. أن الأسلوب الذي استخدم يسمح بالتنبؤ ببداية تولد الدوامة و قوتها وترددها و عدد موجاتها وتوزيع الطاقة بها و كذلك بمنطقه انهيارها.

**ABSTRACT**

Local wavenumber/frequency spectra of pressure fluctuations associated with two types of vortex separation over a prism are examined. The first vortex is a spanwise vortex associated with the separation formed by normal flow over a prism. The second vortex is a conical vortex formed by the separation of a flow at 45° to two sides of the prism. The technique used to estimate the wavenumber-frequency spectra

Accepted July 5, 1999

uses pressure measurements from two taps. For the spanwise vortex, the measurements show that low frequencies and small wavenumbers dominate the pressure fluctuations. Further downstream, the energy is reduced and distributed to a wide range of frequencies and wavenumbers. As for the conical vortex, most of the energy is confined to low frequencies and wavenumbers. Waveuumber spectra for the pressure fluctuations are also presented. The technique used to estimate the wavenumber-frequency spectra is cable to give the vortex formation, its energy distribution and vortex breakdown in space and time.

## INTRODUCTION

Flows over bluff bodies are characterized by separation, vortex formation and breakdown and reattachment regions. In these regions, the turbulenee intensity is very high and the associated turbolence scales extend over several decades. These scales result in strong pressure fluctuations on the surfaee of the bluff body. Time domain analysis such as conditional sampling has been used to characterize significant wall pressure "events" at a point and to relate such events to fluid flow phenomena. Frequency domain analysis has been used to characterize the energy distribution and possibly convection velocities of frequency components of wall-pressure fluctuations. Yet, in many instances, such as flow-induced vibrations and sound generation, time/space and spatial characterization of pressure fluctuations is necessary. Such characteristics, represented in terms of a wavenumber-frequency speetrum, serve as an input to determine the response of structures.

While measurements of temporal Fourier components, i.e. frequencies, can be obtained from time series, measurements of spatial Fourier components, i.e. wavenumbers, require instantaneous sampling at many locations. This is not practical when trying to characterize waveuumber components of pressure fluctuation over bluff bodies. First, obtaining simoltaneous measurements at a large number of taps is not practical. Second, flows over bluff bodies are spatially varying in terms of separation, reattachment or vortex formation and breakdown. Consequently, the associated pressure field is not homogeneous and spatial pressure measurements over a long distanoe could not be used to get the wavenumber spectrum. Thus, a measure of the local wavenumber frequency spectral charaeteristics of pressure fluctuations would be more useful.

The local wavenumber frequency speetrum of pressure fluctuations can be obtained using a technique developed by Beall et al. (1982). That technique uses

simultaneous measurements from two closely spaced points and is based on the recognition that the relation between frequency and wavenumber is stochastic. Jones et al. (1988) used Beall's technique to measure the wavenumber spectrum and dispersion relation in a transitioning plane wake. Hajj et al. (1992) used local wavenumber-frequency measurements to show that matching wavenumber conditions exist between the fundamental and subharmonic frequency components in the region where the subharmonic gains its energy by parametric resonance. Power spectra of wind pressure on low building roofs were measured at various tap location and analyzed by Kumar and Stathopoulos (1998).

In this work, we apply the same technique to obtain wavenumber frequency spectra for the pressure fluctuations associated with the formation of two types of vortices on top of a prism. In the first case, the flow is normal to one side of the prism, which results in flow separation, and formation of a spanwise vortex. In the second case, the flow is at 45° to two sides of the prism. Under these conditions, the flow separation, indueed by the two leading edges at the top of the prism, contains two conical vortices that resemble vortices formed over delta wing aircrafts. Thus, a measure of the local wavenumber frequency spectral characteristics of pressure fluctuations at several location would be more useful to estimate the vortex formation, its energy distribution and vortex breakdown.

**Experimental setup**

The experiments were carried out in the wind tunnel of the ESM Department at Virginia Tech. The tunnel has a test section of 50x50 cm. The tests were conducted at a free stream velocity of 12 m/s with a free stream turbulence intensity equal to 0.5%. The prism (L=10.5 cm, W=8.5 cm and H=8.5 cm) was mounted on the floor of the tunnel. The pressure taps were placed along two directions on the top of the prism as shown in figure 1. The normal direction was used to examine characteristics of pressure fluctuations generated by the flow normal to the prism. Under this flow condition, the flow separates and a spanwise (parallel to the leading edge of the prism) vortex is formed. The pressure taps were set to obtain measurements mostly in the separation region. The 17° direction is used to examine pressure fluctuations under one of the two conical vortices. Based on flow visualization, the conical vortex is formed along this direction when the flow is at an angle of 45° to two sides of the prism. There are 15 pressure taps in each direction. The location of the pressure taps center line are shown in figure 1 and

the distance between each taping are listed in table 1.The pressure taps are coupled with a 24- channel Electronic Pressure Scanner (ESP) which connected directly to the computer through the data acquisition board. Electronic Pressure Scanner interface has the ability to digitally address up to 24 pressure ports. It is 12 bit and 31 kHz analog to digital converter. This conversion speed allows to utilize the full scanning capability of electronic Scanner, which is of the order 20 kHz. The pressure data was acquired with a sampling rate of 125 Hz, which resulted in a Nyquist frequency of 62.5 Hz. The flow visualizations were carried out in the smoke wind tunnel at the Department of Mechanical Engineering at Zagazig University under similar flow conditions to those in the ESM wind tunnel. kerosene are used to generate smoke.

**Methods of Data Analysis:**

The wavenumber frequency spectrum is estimated using the technique introduced by Beall et al. (1982). The technique uses measurements of a fluctuating field such as pressure at two locations separated by a distance $\Delta x$. The measurements are divided into time segments each consisting of N samples. From either of the two records, the auto-power spectrum is computed which provides an estimate of the power associated with a frequency interval $f_i$ and $f_i+\Delta f_i$. Using the two records, the cross-power spectrum is computed. From the phase of the cross-power spectrum $\theta_i(f_i)$, the local wavenumber $K_i(f_i) = \theta_i(f_i)/\Delta x$ is determined. This wavenumber is called local because it is estimated over the separation $\Delta x$ and is different from wavenumbers obtained by applying a spatial Fourier transform to measurements from many spatial locations. The local wavenumber gives a better estimate of spatial characteristics in a spatially varying field, Kumar and Stathopoulos (1998). Having the frequency $f_i$ and an associated local wavenumber, $k_i$, the amount of power, $S(f_i)$, is recorded at the co-ordinate point $(f_i,k_i)$ in the wavenumber frequency, $f$-$k$ plane. Because, there is a stochastic relationship between wavenumber and frequency, every segment may yield different estimates of the power $S(f_i)$ and wavenumber $k_i(f_i)$ for the frequency interval $f_i$ and $f_i+\Delta f$ . The new level of power is entered at a new co-ordinate point consisting of the new value of $k_i$. This process is repeated for all data intervals to obtain the average power, $S_I(k_i, f_i)$, associated with every frequency and every wavenumber in the wavenumber frequency plane. This power is an estimate of the local wavenumber frequency spectrum. The limits of the measured wavenumbers and the resolution are determined by the separation distance between the

pressure taps, $\Delta x$, and the number of grid elements in the wavenumber-frequency domain. The wavenumber that can be obtained are bounded by $-\pi/\Delta x$ and $\pi/\Delta x$. . The wavenumber resolution can be adjusted by setting the number of $k$ cells which in all of our analysis was set at 256. From the local wavenumber frequency spectrum $S_l(k_i, f_i)$, the frequency spectrum $S_f(f_i)$ can be estimated by integrating the spectrum over all wavenumbers, i.e.

$$S_f(f_i) = \Sigma_k S_l(k_i, f_i) \quad (1)$$

and the local wavenumber spectrum $S_k(k)$ can be estimated by integrating the spectrum over all frequencies, i.e.

$$S_k(k) = \Sigma_j S_l(k_i, f_i) \quad (2)$$

The results presented here were obtained from 30 data segments; each segment containing 128 data points and sampled at 125 Hz. This yielded a Nyquist frequency of 62.5 Hz with a frequency resolution of 0.98 Hz. Depending on the measuring location, the separation $\Delta x$ was set at 2.5 or 6.5 mm for the normal flow and it's downstream locations. The separation $\Delta x$ was set at 2.5 or 3.75 mm for the 45° flow and it's downstream locations.

**Results and Discussion**

When the flow is normal to one side of the prism, the flow separates at the sharp corner, forming a separated shear layer, which behaves like a mixing layer and results in the formation of a vortex. Further downstream, the flow curves towards the solid surface (top of prism). As shown in figure 2.a, the flow does not completely reattach although it shows unsteady reversing flow. Those results also showed that there are two important regions in the flow that affect the pressure fluctuations. The first region is where a vortex forms and the second is further downstream where high shear stresses are measured. In the second flow case, the flow is at 45° to two sides of the prism. Under these conditions, there is a three-dimensional separation from the two leading edges at the top of the prism (figure 2.b). The figure shows that the flow on top of the prism consists of two conical vortices in the separation region. These vortices resemble delta- wing vortices. The pressure taps were placed at an angle of 17° to allow for measurements of pressure fluctuations associated with one of the conical vortices

The downstream variations of the frequency power spectrum of the pressure fluctuations in different regions associated with flow separation under normal incidence and the formation of the spanwise vortex are shown in figure 3. Because of the limited

capabilities of the pressure measuring system, the highest analyzed frequency component is 62.5 Hz. The lowest component determined from the record length is 0.98 Hz. Improvements to these measurements, in terms of frequency resolution could have been done yet. Because our interest is in the spatial characteristics of the energy containing components of the frequency spectrum, these limits are satisfactory. The frequency spectra show that at all measuring locations, the level of energy in all frequency components up to 62.5 Hz is more or less constant with a small peak near 10 Hz. Also, the level of energy is slightly smaller in the frequency range between 30 and 60 Hz than between 1 and 30 Hz. The variations in the spectral energy of the pressure fluctuations under the conical vortex are shown in figure 4. In the distance lower than 20 mm the level of energy is slightly higher at frequency range between 1 and 30 Hz. But, In the downstream, x >30 mm the level of energy is distributed at different frequency ranges.

The range of wavenumbers associated with the frequency components shown in figure 3 for the separating region is given in the estimates of $S_f(k, f)$ shown in figure 5. The figures shows local wavenumber-frequency at four downstream locations, x=6.25, 16.25, 26.25 and 46.25 mm. For the locations at x=6.25, 16.25 and 26.25 mm, the separation between the measuring points was 2.5 mm. Thus, wavenumbers between $-12.56$ (1/cm) and 12.56 (1/cm) were measured with a resolution of 0.098 (1/cm). For the location at x=46.25 mm, the separation between the measuring points was 6.5mm which yielded a measure of wavenumbers between $-4.8$ and 4.8 (1/cm) with a resolution of (0.004) (1/cm). Based on figure (2.a), the locations at x=6.25, 16.25, and 26.26 (mm) are in the separation region under the spanwise vortex. The fourth location (x=46.25 mm) falls under the region where bigh shear stresses were measured. There are stroug similarities in the $S_f(k_i, f_i)$ estimates at x=6.25, 16.25, and 26.25mm. At all of these locations, the $S_f(k_i, f_i)$ speetra are narrow and nearly symmetric about the $k=0$ axis for f< 30 Hz. Beyond that frequency, the energy content is relatively negligible. The symmetry around zero indicates that most of tbe fluctuation power is confined to wavenumber that are as small as the cell size, i.e. 0.098 1/cm. At x=46.25 mm, we note two major differences, the level of power at all wavenumbers and frequencies is much smaller than the highest level measured at the locations in the separation region. Moreover, relatively speaking, more power is appearing in the high frequencies These results show that, under the separating spauwise vortex, the main component of the pressure fluctuations has a small wavenumber couponent that, most likely, is associated with the separating vortex. On the other hand,

in the region associated with high turbulence intensity, the pressure fluctuations contain components with large as well as small wavenumbers.

Figure 6 shows estimates of the wavenumber-frequency spectra, $S_I(k_i, f_i)$, of the pressure fluctuations under the conical vortex. The plots are shown for six downstream locations x=10.75, 18.25, 28.25, 38.15, 40.35 and 42.55 mm under the conical vortex. For all of these locations, the separation between the measuring points was set at 3.75 mm. Thus, wavenumbers between –8.4 (1/cm) and 8.4 (1/cm) were measured with a resolution of 0.065 (1/ cm). At x=10.75 mm, most of the energy is contained in the low frequency and low wavenumbers. This indicates that the pressure fluctuations are mostly due to a large- scale structure, i.e. the conical vortex. The same observation holds for the spectrum at x=18.25 and 28.25 mm.. Further downstream, at x=38.15 mm, it is observed that the level of energy at the higher frequencies has increased and that there is a symmetric band of wavenumbers around k=0 that is associated with this energy. At x=40.35 mm and 42.55 mm, the level of energy associated with the low frequencies has dropped significantly. The energy level of the high frequency components has increased and the width of the band of wavenumbers associated with these components has also increased. This indicates that the pressure fluctuations are still affected by the conical vortex. On the other hand, there are other components with higher frequency and wavenumbers. These components can be related to turbulence structures around the conical vortex. These structures have a smaller scale than the conical vortex. The expansion of energy into the higher frequency and wavenumber components indicates the beginning of the breakdown of the conical vortex.

Wavenumber spectra of the pressure fluctuations in the different regions associated with flow separation under normal incidence and the formation of the spanwise vortex and obtained by integrating the wavenumber frequency spectra are shown in figure (7). At x=6.25, 16.25 and 26.25 mm, the levels of energy at all wavenumbers are similar. We note also the (-1) slope observed for the wavenumbers between 0.2 and 2.0 (1/cm). This slope is noted because it has been observed in wavenumber spectra of pressure fluctuations associated with boundary layers. On the other hand, at x=46.25 mm, the level of power at the low wavenumbers (<0.2 $m^{-1}$) remains the same while it is much lower at the higher wavenumbers. These results indicate that under the separation vortex, the power is mostly confined to a small range of wavenumbers at frequencies. On the other hand, under the high turbulence region, the

power at all wavenumbers is lower than that under the vortex. Figure (8) shows wavenumber spectra of the velocity fluctuations under the conical vortex at six locations. The results show that the level of energy at all wavenumbers is almost the same at the first five locations. By the last location, the level has slightly decreased. We note also the (-1) slope observed for the wavenumbers between 0.4 and 4.0 (1/cm) at all locations.

**Conclusions**

Using pressure measurements from two taps, we were able to present estimates of local wavenumber frequency spectra under two types of vortices associated with separation regions over bluff bodies. The first vortex is a spanwise vortex formed on top of a prism as a result of a normal flow. The measurements show that right under the spanwise vortex, low frequencies and small wavenumbers dominate the pressure fluctuations. The pressure fluctuations in this region are mostly affected by the vortex. Further downstream, where the shear stresses are high, the total energy is reduced and is distributed to a wide range of frequencies and wavenumbers. The pressure fluctuations are affected by a wide range of turbulence structures. The second vortex is a conical vortex formed by the separation caused by a flow at 45° to two sides of the prism. Throughout the region under the vortex, most of the energy is confined to low frequencies and wavenumbers. Only when the smaller scales of turbulent structures form around the vortex, the energy expands into higher frequencies and wavenumbers. Wavenumber spectra, estimated by integrating the wavenumber frequency spectrum, show that most of the energy is contained by the small wavenumbers.

**References**

Beall, J.M., Kim,Y.C., and Powers, E.J., 1982 "Estimation of wave number and Freqnency Spectra Using Fixed Probe Pairs" Journal Applied Physics Vol. 53, pp.3933-3940.

Jones, F.L., Ritz, Ch. P., Miksad, R.W., Powers, E. J., and Solis, R. S., 1988 "Measnrement of local wave number and frequency spectrum in a plane wake" Journal Experiment fluids Vol. 6, pp.365-372.

Kumar, K.S. and Stathopoulos, T., 1998 "Power spectra of wind pressures on low building roofs" J. of Wind Engineering and Industrial Aerodynamic Vol. 74-76, pp. 665-674.

Hajj, M. R., Miksad, R. W. and Powers, E. J. 1992, "Subharmonic growth by parametric resonance" Journal Fluid Mech. Vol. 236, pp.385-413.

| points | distance | |
|---|---|---|
| | 90 ° | 45 ° |
| 0-1 | 5 | 9.5 |
| 1-2 | 2.5 | 2.5 |
| 2-3 | 2.5 | 2.5 |
| 3-4 | 2.5 | 2.5 |
| 4-5 | 2.5 | 2.5 |
| 5-6 | 2.5 | 2.5 |
| 6.5 | 2.5 | 2.5 |
| 7-8 | 2.5 | 2.5 |
| 8-9 | 2.5 | 2.5 |
| 9-10 | 2.5 | 3.75 |
| 10-11 | 6.5 | 3.75 |
| 11-12 | 6.5 | 2.5 |
| 12-13 | 6.5 | 2.5 |
| 13-14 | 6.5 | 2.5 |
| 14-15 | 6.5 | 2.5 |

Table (1) Distance between measuring points

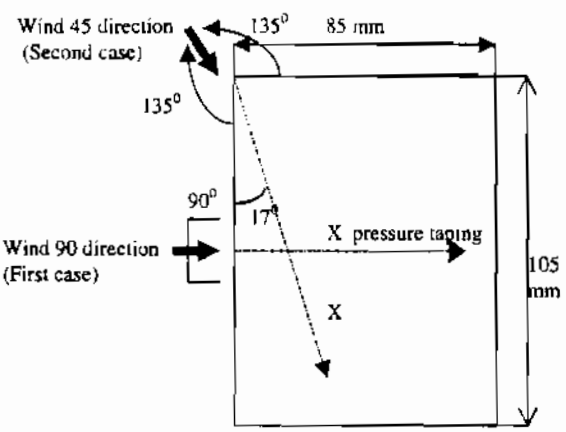


Fig. (1) Prism Dimension and pressure taping center line, (105x85x85 mm).

Fig. (2.a) Flow upon prism with 90 degree angle

Fig. (2.b) Flow upon prism with 45 degree angle

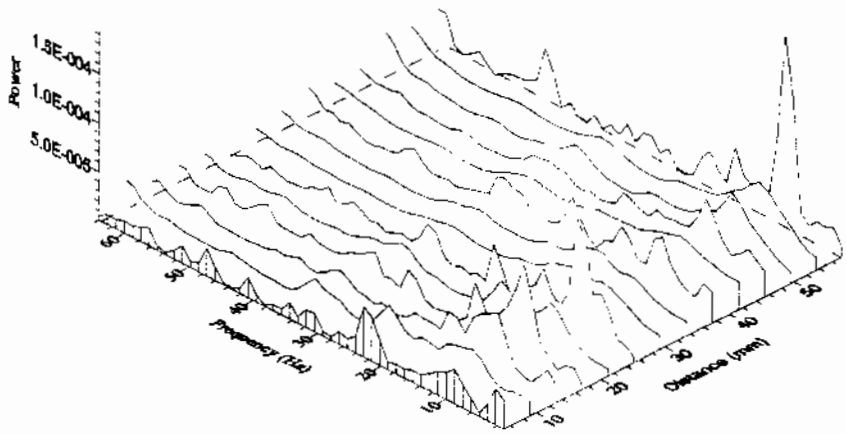


Figure 3. Frequency spectrum at various locations under spanwise vortex

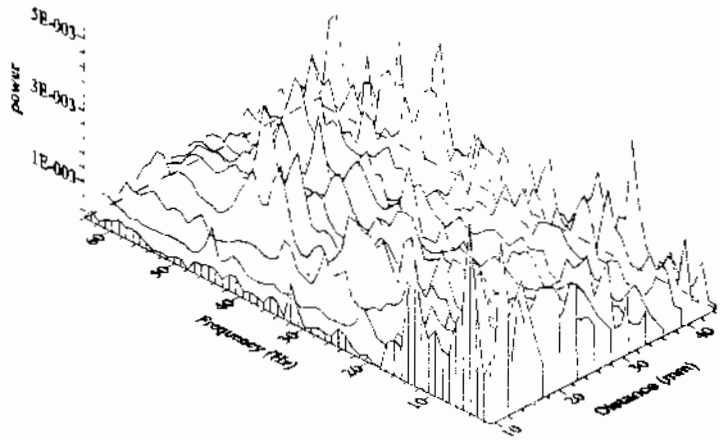


Figure 4. Frequency spectrum at various locations under the conical vortex

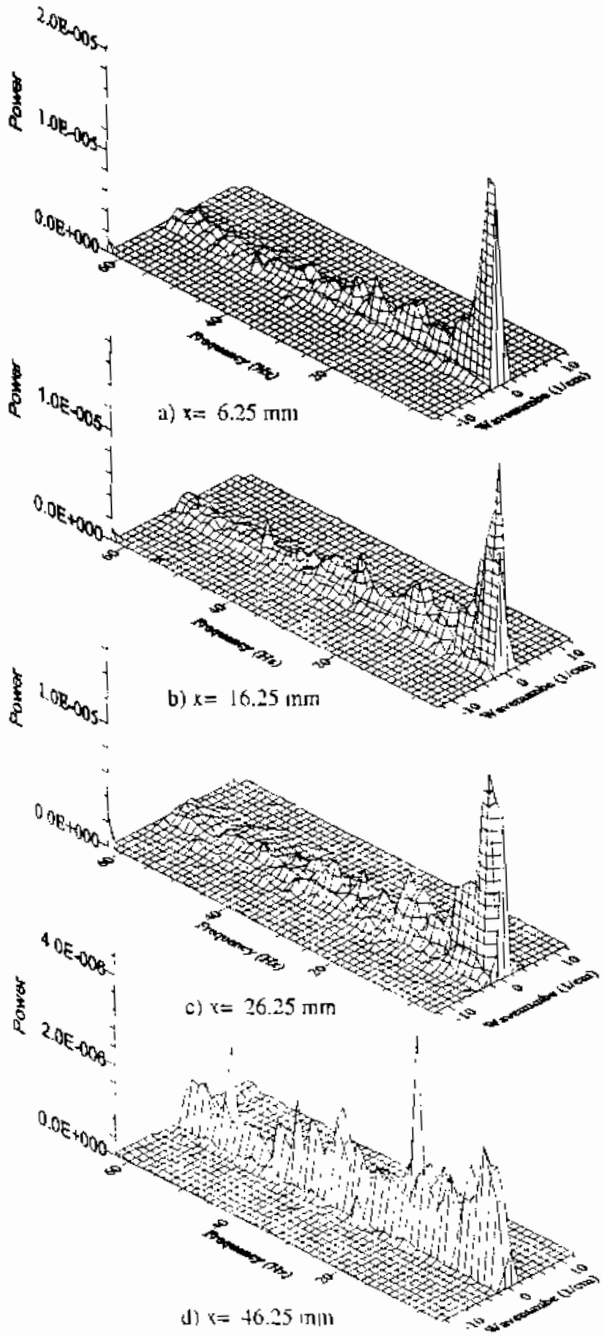


Figure 5. Wavenumber – frequency spectra at different locations in the separation region associated with normal flow

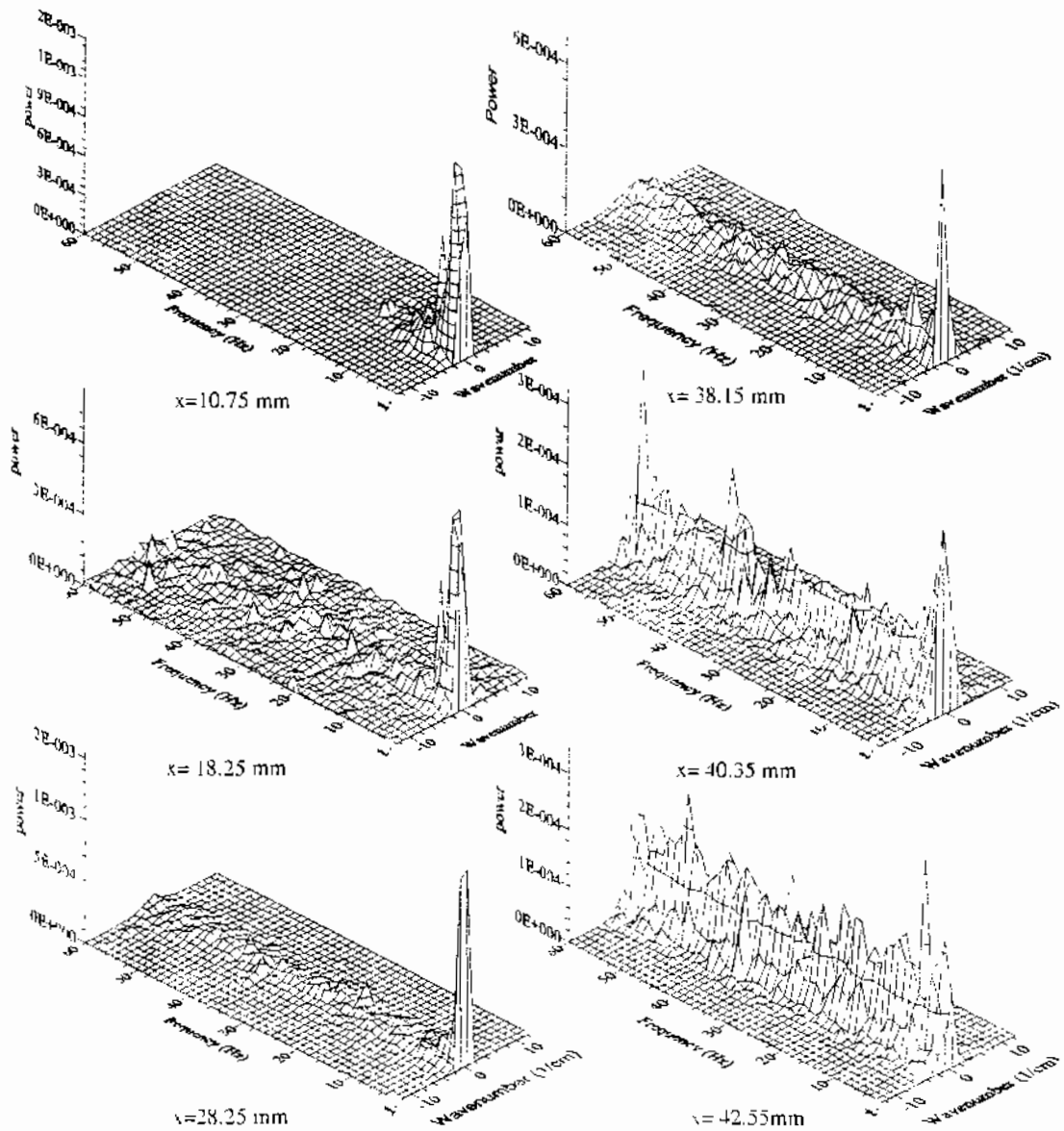


Figure 6. Wavenumber - frequency spectra at different locations unde the conical vortex

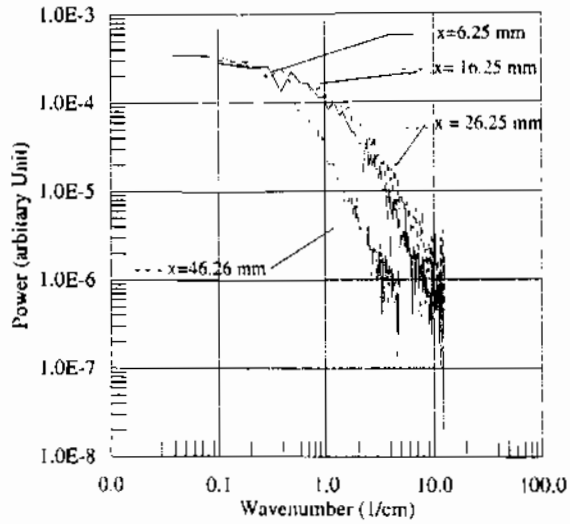


Figure 7. Wavenumber spectra in the separation region under normal flow direction.

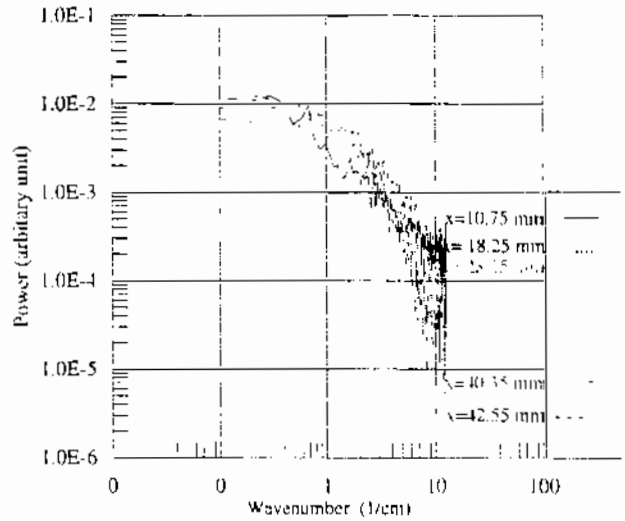


Figure 8. Wavenumber spectra under the conical vortex